Hybrid Simulations of Hall Thrusters Operating on Various Propellants

IEPC-2009-075

Presented at the 31st International Electric Propulsion Conference,
University of Michigan • Ann Arbor, Michigan • USA
September 20 – 24, 2009

Eunsun Cha[1], David B. Scharfe[2], Michelle K. Scharfe[3], and Mark A. Cappelli[4]
Stanford University, Stanford, CA, 94305

and

Eduardo Fernandez[5]
Eckerd College, St. Petersburg, FL, 33711

Abstract: Bismuth, krypton and molecular nitrogen are examined, by way of computer simulation, as alternative propellants for Hall thruster operation. Based on the simulated results of a laboratory Hall thruster operating on xenon, a shear-based transport model is extended to the operation of a similar thruster with these alternative propellants, and modifications are made in the thruster designs to examine the sensitivity of computed performance to design parameters. We compare computed performance for krypton to that of xenon in identical thruster geometries. We also examine the performance of this thruster on bismuth for geometries of varying channel lengths, and performance on nitrogen with varying magnetic field distribution.

Nomenclature

B	=	magnetic field (T)
E	=	electric field strength (V/m)
N	=	neutral number density (m^{-3})
s	=	shear rate (sec^{-1})
u	=	velocity (m/s)
$\omega\tau$	=	Hall parameter
I_{sp}	=	specific impulse (sec)
η	=	thrust efficiency (%)
T	=	thrust (N)
P	=	power (W)
x	=	dimensionless electron temperature
U_i	=	ionization energy (eV)
ϕ_c	=	ionization energy cost (eV)
α	=	Townsend ionization coefficient (m^{-1})
Subscripts		
eff	=	effective

[1] Research Assistant, Mechanical Engineering Department, escha@stanford.edu
[2] Research Assistant, Mechanical Engineering Department, scharfe@stanford.edu
[3] Research Assistant, Mechanical Engineering Department, mkallis@stanford.edu
[4] Professor, Mechanical Engineering Department, cap@stanford.edu
[5] Associate Professor, Mathematics and Physics, fernane@eckerd.edu

clas = classical
nw = near wall
fluc = fluctuation
r = radial direction
z = axial direction
θ = azimuthal direction
Xe = xenon
N_2 = molecular nitrogen

I. Introduction

HALL thrusters have been widely used in satellite station keeping applications. More recently, the European SMART-1 mission demonstrated the capability of Hall thruster electric propulsion as a main propulsion option for lunar missions, and also demonstrated its potential for deep space or interplanetary missions.[1] These past successful Hall thruster applications use xenon as a propellant. Xenon has several advantages over other propellants because of its chemical inertness, low ionization energy, relatively high atomic mass, and storability, however, its scarcity and resulting high cost (as high as about \$850/kg[2]) has led to the serious examination of alternative propellant options, particularly for missions that require high propellant throughput.

Other attractive propellants that have been considered for Hall thruster electric propulsion include bismuth and krypton.[2,3]

Bismuth has several advantages as a propellant. Besides its abundance and low price (approximately one thousand times less expensive than xenon) it is the heaviest of all radioactively-stable atoms, with an atomic mass of 208.98 amu. Since thrust scales as the square root of the propellant atomic mass,[3] a thruster operating on bismuth has the potential to provide the maximum thrust at a given power. Bismuth has several properties that make it easier to ionize than xenon, including a low ionization potential energy (7.3 eV to 12.1 eV for xenon), a relatively low ionization cost and a high ionization probability – all are expected to enhance thruster performance. Furthermore, bismuth is a solid metal at room temperature thereby resulting in a potentially high pumping capacity in laboratory testing, better reproducing space conditions. The condensable property of bismuth provides easier handling and on-board storability. However, these properties may also adversely affect spacecraft integration, as this condensability causes bismuth to coat any surface that the source may be exposed to, resulting in considerable concerns about spacecraft contamination.

Krypton is an attractive Hall thruster propellant because it shares similar properties to xenon, perhaps more so than any other alternatives. It is also an inert noble gas, but it is approximately ten times less expensive than xenon. In most of the present electrostatic thrusters designed for xenon propellant, switching to krypton propellant would lead to minor costs in spacecraft re-qualification. Since krypton has a lighter mass than xenon (83.30 amu to 131.29 amu of xenon) and a slightly higher ionization potential, performance on krypton operation is expected to be slightly worse than that on xenon. Generally lower thrust efficiencies have been seen in prior comparisons.[3] It is noteworthy, however, that in almost all of these prior comparisons, studies were carried out on thrusters that were initially optimized on xenon. The lighter mass is expected to lead to higher specific impulse, I_{sp}, which is desirable in some applications; but such an option would impose a thrust to power (T/P) penalty, and is of interest in applications where power is not limited. It is interesting to note that not all of the prior comparisons to xenon resulted in higher

Propellant	N_2	Kr	Xe	Bi
Atomic Mass [amu]	28.01	83.8	131.29	208.98
Ionization Energy [eV]	15.6	14.0	12.12	7.29
First Excitation [eV]	6.17	9.92	8.32	4.04
Abundance	79 mol % in air	1.14 ppm in air	0.087 ppm in air	Abundant mineral
Element Type	Molecular gas	Noble gas	Noble gas	Metal
State at STP	Gas	Gas	Gas	Solid
Relative Cost	Not a Factor	Moderate	High	Low
Handling Complications	No	No	No	No

Table 1. Properties of N_2, Kr, Xe, Bi propellants.

I_{sp}.[3]

In addition to the interest paid to these heavy atomic propellants, our laboratory has examined the possibility of using molecular nitrogen (N_2) as a Hall thruster propellant for particular applications. Molecular nitrogen is a major mass carrier in the by-product of hydrazine decomposition. One might envision a spacecraft dual-mode propulsion system, with hydrazine chemical or arcjet thrusters providing the high *T/P* option, and hydrazine decomposition product Hall thrusters providing a high I_{sp}, option, both using a common propellant system. The development of Hall thrusters capable of running on air opens up intriguing possibilities for air-breathing electric propulsion in very low earth orbit applications.

Nitrogen is one of the most abundant elements on earth, comprising 79% of air (per mole) in its molecular form (N_2). Also, nitrogen is relatively stable, with a dissociation energy of 9.8 eV. In comparison to xenon, it has a relatively high ionization energy (15.6 eV to 12.1 eV for xenon), a lower ionization cross section, and higher ionization cost factor due to its molecular structure. The lower molecular mass of nitrogen also introduces an obstacle to efficient ionization, because of its higher thermal velocity, resulting in a shorter residence time within the thruster channel and, particularly, in the region where ionization of propellant takes place.

Our objective in this paper is to review our activities on computer-based simulations of Hall thrusters operating on molecular nitrogen, bismuth and krypton, and to demonstrate the possibility of the use of these simulations in guiding the development of advanced thruster designs. A two-dimensional (2D) hybrid particle-in-cell (PIC) simulation was employed and modified to evaluate each propellant, details for which will be presented in Section II. In particular, we model transport using the shear-based mobility derived from comparing xenon Hall thruster simulations to experiments, as described by Scharfe.[4] We assume that this higher-order transport model is more transportable to other thruster configurations or propellants than other ad-hoc transport coefficients, such as Bohm diffusion, and it appears to capture the transport barrier often seen in these devices, close to the exit plane, where there is a strong axial shear of the azimuthal electron velocity. An examination of how this shear-based model performs on thrusters operating on these three propellants (nitrogen, krypton, and bismuth) will be presented in Section III.

II. Numerical Model

A. Hybrid simulation and shear-based transport model

The hybrid PIC simulation used to investigate the various Hall thruster operating benefits for these propellants is a radial-axial hybrid model of the interior channel and near field region of a laboratory Hall thruster (Stanford Hall Thruster-SHT).[5,6] The simulated geometry corresponds to an annular thruster channel 8 cm in length, 1.2 cm in width, and with an outer diameter of approximately 9 cm, graphically depicted in Fig. 1a. The imposed magnetic

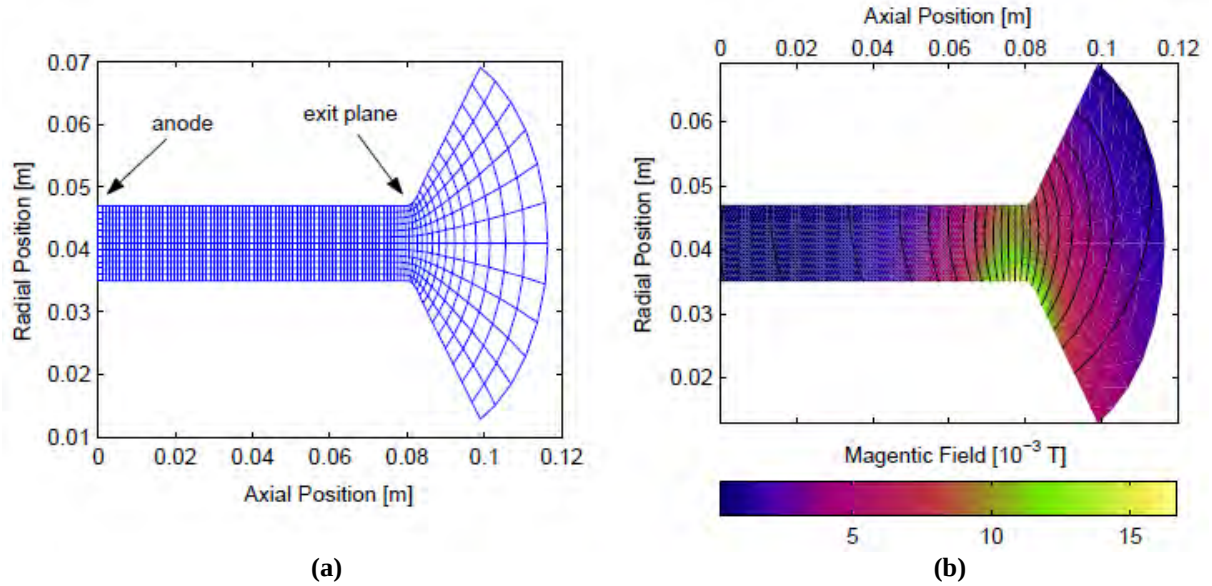

Figure 1. (a) Computational grid of the Stanford Hall Thruster radial-axial simulation. (b) Magnetic field strength and contour lines of the Stanford Hall Thruster.

field shown in Fig. 1b agrees reasonably well with measurements taken along the channel centerline. We assume that the Hall thruster discharge itself, through the development and fluctuation of the Hall current, does not significantly affect the magnetic field within the channel.[3]

The hybrid PIC simulation[7] treats electrons as a quasi-one-dimensional (direction normal to the magnetic field lines) fluid governed by the first three moments of the Boltzmann equation while ions and neutrals are modeled as superparticles, using a particle-in-cell (PIC) approach similar to the model first proposed by Fife.[8] The ions and electrons are coupled through an assumption of quasi-neutrality. This releases the electron continuity equation to define the B-field-normal electron velocity. The *B*-field normal momentum equation is used to calculate the electric field. The electron energy equation is then used to determine the electron temperature. The electron temperature is taken to be constant along the magnetic field lines.

Neutral superparticles are injected from the center of the anode based on the prescribed mass flow rate and are ionized by electron-impact ionization to produce singly-ionized atoms/molecules. The ionization process is modeled as a probability function of electron temperature and in addition to serving as a source in the electron continuity equation, also serves as an energy drain in the electron energy equation. The energy lost through ionization includes cost-factors to indirectly account for non-ionizing collisions which ultimately result in internal energy and radiation losses. The heavy particle species are advanced in time through solution of their respective equations of motion in cylindrical coordinates. For xenon, the simulation is initialized with approximately 500,000 neutral superparticles and 200,000 ion superparticles, where each superparticle represents between 10^8 and 10^{12} actual particles.[4] Although previous research by our group has examined the role played by charge exchange collisions and the finite background gas pressure[9], these effects are not included in the results presented in this study.

The electron transport model is a semi-empirical model[4] that attempts to account for the suppression of transport-causing fluctuations by the strong shearing in the electron fluid along the cross-field direction in regions of strong magnetic field. Our model is motivated in part by successes of similar models in the study of particle transport in high temperature plasmas, and also by the dynamical behavior of the linearized fluid equations for a Hall thruster.[10] The model we use is of the form:

$$\left(\omega\tau\right)_{eff}^{-1} = \left(\omega\tau\right)_{clas}^{-1} + \left(\omega\tau\right)_{nw}^{-1} + \left(\omega\tau\right)_{fluc}^{-1}\left(\frac{1}{1+\left(Cs\right)^2}\right) \tag{1}$$

where $\omega\tau_{clas}$ is the classical Hall parameter based on electron neutral collisions, $\omega\tau_{nw}$ is the near-wall term based on the electron collisions with the channel walls, $\omega\tau_{fluc}$ describes the transport due to fluctuations, and the shear rate, s, is given by:

$$s = \frac{du_{e,\theta}}{dz} = \frac{dE_z/B_r}{dz} \tag{2}$$

Details of this model can be found in Thomas.[10] In the study presented here, $\omega\tau_{fluc}$ is treated as a parameter, taken to be close to (but not exactly) the commonly used Bohm[11] value of 16. Also, the coefficient C which can be thought to represent a turbulence decorrelation time in the absence of shear, is treated as a parameter. These parameters are generally obtained by comparing computed plasma properties for operation of the SHT on xenon to those measured experimentally.[4] As shown in Scharfe,[4] the results are moderately sensitive to the selection of both parameters. We surmise, however, that this higher-order transport model is more transportable amongst thrusters of different geometries and different operating conditions than a simple Bohm transport description, and is expected to respond to variations in discharge voltage, as past experiments have shown that the strength of the transport barrier increases with increasing voltage.[6]

While incorporating this model into the hybrid simulation, three assumptions are made to reduce computational cost and increase numerical stability. First, the Hall parameter is only calculated along the center of the channel and is assumed to be radially uniform. Second, the Hall parameter outside of the channel (beyond the exit plane, $z = 0.08$ m) is assumed to be constant at the value specified by the fitting parameter, $\omega\tau_{fluc}$. This assumption is supported by recent kinetic simulations,[12] which indicate that electron collisions with the outer thruster wall can lead to highly non-local, even super-Bohm levels of transport. Lastly, the updating of the effective Hall parameter is under-relaxed, resulting in an instantaneous Hall parameter that contains remnant effects from the previous 1000 time steps.[4]

B. Basic code modification

The simulation for each propellant alternative evolved from the hybrid simulation suited for xenon in a gradual way. This was found to be necessary in order to prevent numerical instabilities from evolving to the point where unphysical values in parameters were obtained. For every propellant, the atomic weight of the propellant was first altered. Then, the ionization threshold energy (shown in Table 1) was changed, which was followed by the modification of the ionization probability as a function of the electron temperature. Like our xenon simulations, only single ionization is assumed to take place and volume recombination processes are not considered. Note that for nitrogen ionization, only direct molecular ionization ($e^- + N_2 \rightarrow N_2^+ + 2e^-$) was assumed; i.e., any dissociation, dissociative ionization, and direct atomic ionization ($e^- + N \rightarrow N^+ + 2e^-$) was not considered. This is justified as the residence time of injected molecular nitrogen in the thruster channel, in particular, in the region where the electron impact take place, is much shorter than the time needed for both dissociation and atomic ionization to take place. Therefore N^+ ions and N atoms are expected to exist at very low level and are not considered in the present analysis. Experimental measurements on Hall thrusters operating on nitrogen propellant are currently ongoing to verify this assumption.

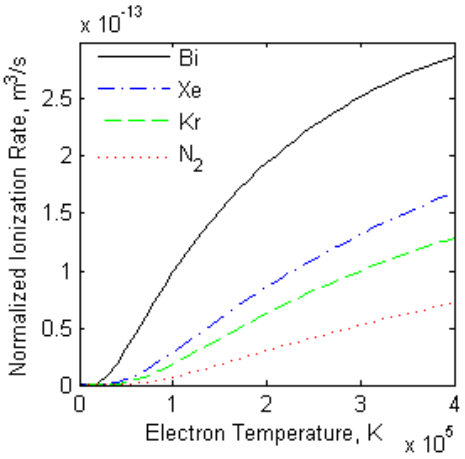

Figure 2. Ionization rate for bismuth, xenon, krypton and nitrogen.

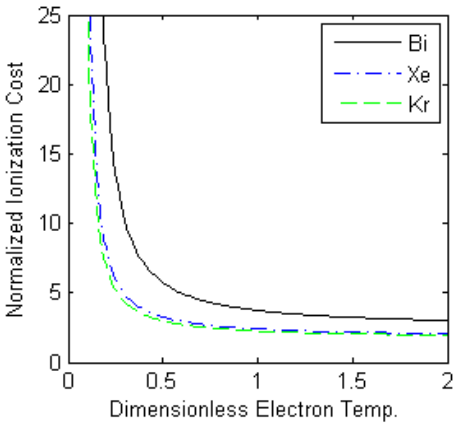

Figure 3. Ionization cost factors of bismuth, xenon, and krypton.

Experimentally measured cross sections[13,14] of electron-impact ionization for bismuth and krypton were used to obtain the ionization rate as a function of electron temperature, and the Binary-Encounter-Bethe (BEB) model[15,16] was used to calculate nitrogen ionization cross section for subsequent determination of the ionization rate, as shown in Fig. 2. As discussed in Section I, the ionization rate of bismuth is significantly higher than that of xenon, while those of nitrogen and krypton are significantly lower.

The ionization cost factor (representing the energy lost from the electron pool during a typical ionization event due to non-ionizing collision processes) for bismuth and krypton are modeled following the method of Dugan[17] assuming that the dominant energy loss mechanism is the excitation of the first (resonance) electronic states. The cost factor, ϕ_c, for bismuth has the following form:

$$\phi_c' = \frac{\phi_c}{U_i} = 2.3895 e^{\frac{0.4340}{x}} + 0.0440 \tag{3}$$

where x is the dimensionless electron temperature, normalized by the ionization energy U_i. For krypton we use:

$$\phi_c' = \frac{\phi_c}{U_i} = 1.6576 e^{\frac{0.2855}{x}} + 0.0476 \tag{4}$$

Since nitrogen has a more complex electronic, vibrational, and rotational structure, we use an alternative approach to estimate the ionization cost factor. We define the ionization cost, ϕ_c, as the electron energy lost per newly produced electron. It can be related to the Townsend ionization coefficient α, which depends on the reduced electric field E/N. The ionization cost (expressed in eV when the field is expressed in Volts) is given as,[18,19]

$$\phi_c = \frac{E}{\alpha} = \frac{(E/N)}{(\alpha/N)} \tag{5}$$

We use the Boltzmann equation solver, BOLSIG[20], to obtain steady-state values for ϕ_c, for both xenon and N_2 at values of E/N ranging from 10^2 - 10^7 Td (where 1 Td = 10^{-17} V·cm^2) – the operating range of the simulation. The ratio of ϕ_c of nitrogen to ϕ_c of xenon is evaluated over this range of E/N, and then multiplied by the ionization cost factor of xenon determined using the method of Dugan[17] (see Fig. 3), to obtain the temperature dependence. The ratio $\phi_{c,N2}/\phi_{c,Xe}$ is plotted in Fig. 4, and the sensitivity of the simulation to this multiplication is found to be rather small. The one drawback of this method is that the electron energy distribution used in evaluating the Townsend coefficients do not account for the magnetized nature of the electrons.

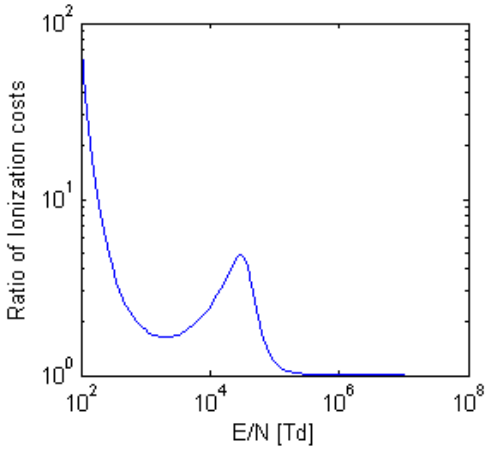

Figure 4. Ratio of the ionization cost of nitrogen to that of xenon.

As mentioned earlier, the shear-based transport model is applied to all three propellant simulations. Previous experience on using this model for xenon indicated that the overall results are only moderately sensitive to the parameters C and $\omega\tau_{\text{fluc}}$ as they are varied by over an order of magnitude. The values used for the bismuth and krypton studies were equal to those established as benchmarks from the xenon studies ($\omega\tau_{fluc}$ = 8, C = 16 × 10^{-8} sec). Use of these values for nitrogen led to problems with numerical stability, and for the results presented here, we use slightly lower values of each ($\omega\tau_{fluc}$ = 5, C = 2 × 10^{-8} sec).

As described in Sec. III below, the initial results of the simulations suggested thruster modifications for improved performance, such as a reduction in channel length (for bismuth) and a broadening of the magnetic field distribution (for nitrogen) when compared to the nominal thruster configuration.

III. Results and Discussion

A. Bismuth

A comparison of the time-averaged plasma density computed for the SHT operating on xenon (top) and bismuth (bottom) at a discharge voltage of 200 V are shown in Fig. 5. As seen in these color-maps, the bismuth thruster benefits from the higher ionization probability, resulting in nearly an order of magnitude larger plasma (ion/electron) density. It is also seen that the ionization zone is displaced, moving closer to the anode. The upstream ionization in this extended channel design is a source of inefficiency, as bismuth ions are likely to collide with the wall and recombine into neutrals prior to exiting the channel. The result shown corresponds to a thrust efficiency of 27% compared to a value of 31% for xenon. Under optimum conditions, we would expect a higher thrust efficiency for bismuth.

Motivated by the lower computed bismuth thrust efficiency for the benchmark geometry, a modified design concept that progressively shortens the channel length

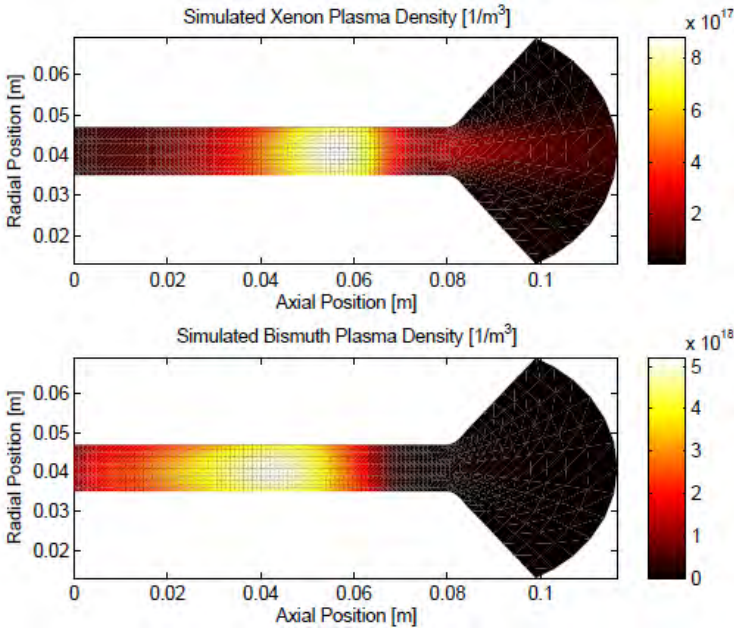

Figure 5. Comparison of time-averaged plasma density for simulated SHT operating on xenon and bismuth propellant.

Propellant	Channel, cm	Thrust, mN	Current, A	I_{sp}, s	η, %	T/P, mN/kW
Xe	8	23.2	3.39	1186	19.9	34.3
	2.4	24.4	3.81	1248	19.5	32.1
Bi	8	18.9	2.11	606	13.3	44.7
	3.3	31.1	3.95	996	19.3	39.3
	2.4	32.6	3.27	1046	25.5	49.9

Table 2. Performance summary for xenon (2mg/s) and bismuth (3.18 mg/s) simulations.

was adopted. Modifications were made by truncating computational cells inside the channel. In the first analysis, 50 axial cells were removed from the anode side of the channel to simulate a Hall thruster of otherwise the same configuration but with a 3.3 cm channel length. A subsequent analysis removed 10 more to reduce the channel length to 2.4 cm.

The results of these simulations are compared in Table. 2. These comparisons use the same propellant anode particle flux (2 mg/s for xenon and 3.2 mg/s for bismuth). Overall, the simulations indicate that when operating on xenon, the performance is rather insensitive to the channel length. In contrast, a considerable sensitivity is seen when operating on bismuth. Note also that the thrust (T), specific impulse (I_{sp}), and efficiency (η) are especially low for bismuth (in comparison to those for xenon) for the extended (8cm) channel. However, the overall performance improves for bismuth as the channel length is shortened. The 2.4 cm channel length thruster operating on bismuth is predicted to outperform that operating on xenon, with a higher thrust efficiency at a slightly lower power, and a lower specific impulse (much higher T/P ratio).

B. Krypton

Krypton simulations were carried out in the nominal (8 cm long) extended channel configuration, but at two different mass flow rates – 2 mg/s (matching the mass flux of xenon), and 1.28 mg/s (matching number flux of xenon). All the basic modifications that characterize krypton properties are applied as well as the shear-based transport model with $\omega\tau_{fluc} = 8$, and $C = 16 \times 10^{-8}$ sec. As expected, due to krypton's lower atomic mass, the axial ion and neutral velocities are much higher than those of xenon. The computed plasma density (at a mass flow of 1.28 mg/s) is compared to that of xenon in Fig. 6. As expected, the density is lower, primarily due to the increased velocity, but also because of the reduced ionization fraction resulting from the higher ionization cost and ionization potential. The overall summary results of the krypton cases are compared to those of xenon in Table 3. The performance parameters with krypton, namely thrust, discharge current, specific impulse, and total efficiency are all notably lower for the 1.28 mg/s mass flux case than for the 2 mg/s case. A

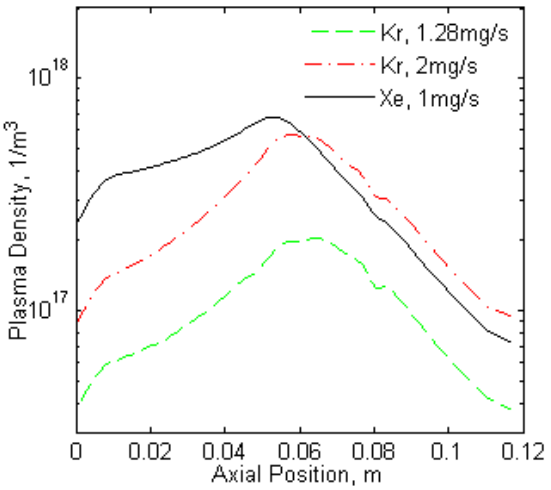

Figure 6. Comparison of plasma density of the SHT simulations on xenon 2mg/s and krypton 1.28mg/s, and 2mg/s.

Propellant	Mass Flow, mg/s	Thrust, mN	Current, A	I_{sp}, s	η, %	T/P, mN/kW
Xenon	2.0	23.2	3.39	1186	19.9	34.3
Krypton	2.0	24.7	3.84	1264	19.9	32.2
	1.28	10.4	1.49	831	14.2	34.9

Table 3. Performance summary for krypton simulations with two mass flow rates, compared to standard xenon SHT simulation.

comparison of the 2 mg/s case to that of xenon reveals a rather surprising result – with the exception of the thrust to power ratio, all of the properties are equal to or greater than those of xenon. This result suggests that the extended channel added a favorable benefit on krypton operation, providing a longer residence time within the ionization region of the discharge.

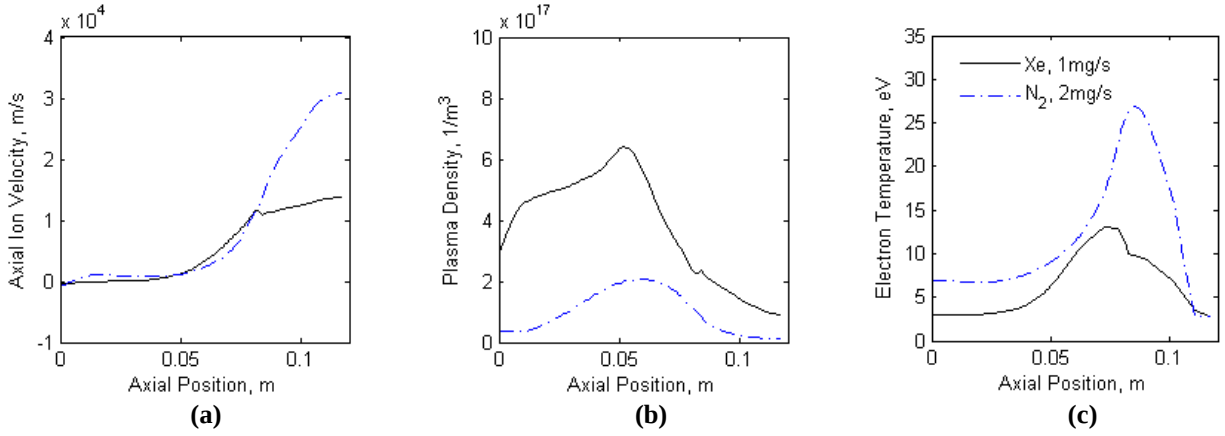

Figure 7. Comparison of (a) axial ion velocity, (b) plasma density, and (c) electron temperature for the SHT

C. Nitrogen

The simulation was also modified for operation on nitrogen as described previously. The particle mass was decreased to 28 amu, the ionization potential was increased to 15.6 eV, the changes were made to the ionization rate (see Fig. 2) and ionization cost factor together. Once again, the shear-based transport model is used for electron mobility. Initial runs were carried out at a mass flow rate of 1 mg/s to match the anode neutral density, and a discharge voltage of 200 V. The shear-based transport model was used with parameters of $\omega\tau_{fluc} = 5$ and $C = 2 \times 10^{-8}$ sec.

The results of the simulations with the base geometry (8 cm channel and standard magnetic field profile) are as expected (see Fig. 7). The exit plane ion velocity is about twice that of xenon ions, while the plasma density is five times lower in its peak, despite comparable electron temperatures. Like that of krypton operation, this is in part due to the higher ion velocity, and to a substantially reduced ion fraction. Examination of the axial velocity profile suggests that the nitrogen ions are not fully accelerated before they exit the channel, and that the region where the electron temperature peaks is pushed toward the exit of the channel. This results in an overall poor performance, with a thrust of $T = 6.9$ mN, and thrust efficiency of $\eta = 3.7\%$. This is not unexpected from the lower atomic mass and ionization properties. The relatively high thermal velocity of

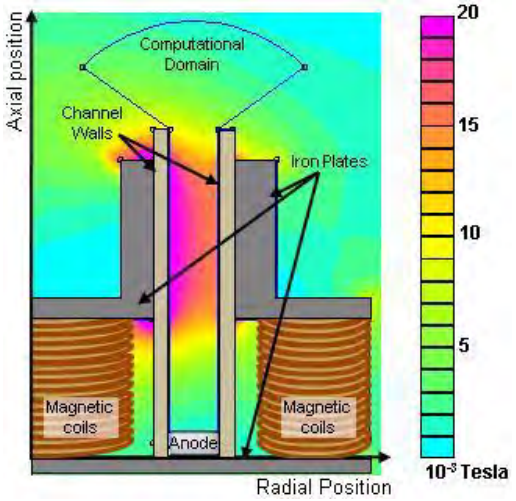

Figure 8. FEMM generated Magnetic field profiles of modified SHT design for nitrogen.

Magnetic Field	Mass Flow, mg/s	Thrust, mN	Current, A	I_{sp}, s	η, %	T/P, mN/kW
SHT	1	6.8	3.1	692	3.7	9.19
Modified	1	12.3	5.2	1324	7.3	8.42
	1.5	24.4	10.5	1662	9.5	12.84
	2	38.6	16.5	1971	11.3	11.68

Table 4. Performance summary for nitrogen simulations with two mass flow rates with the modified B-field, compared to 1 mg/s simulation with SHT B-field.

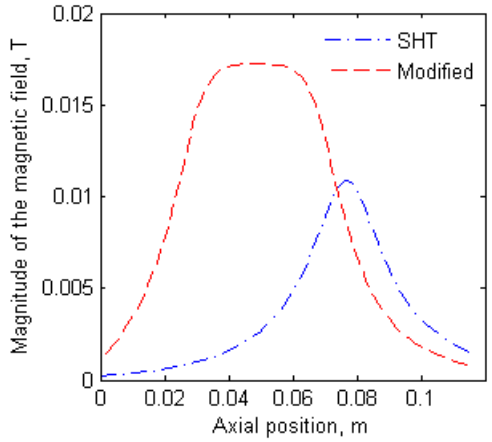

Figure 9. Magnetic field profiles of SHT and modified design for nitrogen.

neutral nitrogen causes molecules to have considerably lower residence time within the channel, resulting in poor propellant utilization. It is clear that a thruster optimized for one propellant must be reconfigured to operate on another. Improvement in performance on nitrogen will require broadening the magnetic field profile to provide a larger region of ionization during neutral transit through the channel.

To guide future experimental design, modifications were made to the standard SHT magnetic circuit, to provide a more intense and wider magnetic field profile along the channel (see Fig. 8). Relative to the original design, the magnetic poles were shortened and the usual magnetic pole plate on top of the thruster channel was replaced with a thick-walled co-axial annular cylinder. The channel length was preserved in comparison to the original design. The resulting magnetic field is visualized by the color map in Fig.8. Field simulations were estimated using Finite Element Method Magnetics (FEMM), an open-source software package.[21] The simulated centerline magnetic field magnitude is compared to that of the nominal SHT design in Fig. 9.

The plasma potential distribution with this modified magnetic field is compared to the original SHT field design in Fig. 10. We see that as the peak of the magnetic field is widened, the potential falls more gradually moving from the anode to the cathode-side. Ionization is likely to occur further within the channel, and an improvement in propellant utilization is expected. Figure 11 compares computed plasma density. We see that with the modified magnetic field profile, there is an increase in plasma density by as much as 50%, reflecting an increase in ionization efficiency. Consequentially, performance is also improved as summarized in Table 4. The field modification at a flow rate of 1 mg/s results in a thrust improvement by as much as 81%, an increase in I_{sp} by as much as 91%, and an almost doubling in efficiency.

Motivated by the improvements achieved with the modified design, further simulations were carried out at increased nitrogen mass flow rates (1.5 mg/s and 2 mg/s). It is clear from the results provided in the table that operating at higher flow rates greatly improves performance. The increased benefit associated with increased mass flow rate is attributed to the higher neutral number density within the channel, promoting increased ionization rates. The highest flow rate illustrated in Table 4 shows an overall increase in discharge current, plasma density, and efficiency, with thrust increasing to 38.6 mN, the I_{sp} increasing to 1971 sec, and a thrust efficiency in excess of 10%. Further studies will continue to examine design changes (such as a smaller channel area, resulting in higher number densities) that may yield further improvements in efficiency.

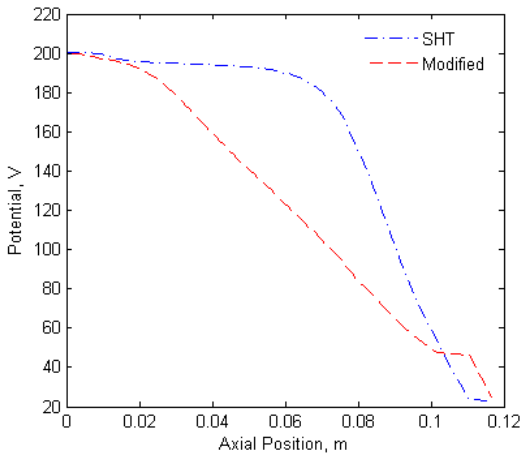

Figure 10. Axial potential variation for the nominal SHT case (on nitrogen) and that with the modified B-field simulations.

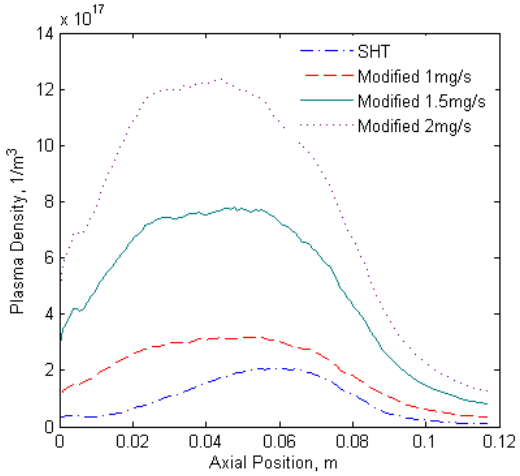

Figure 11. Plasma density of the nominal SHT case and the modified B-field simulations.

IV. Conclusion

Computational studies aimed at comparing Hall thruster performance on bismuth, krypton, and molecular nitrogen are presented. The results indicate that shortening the channel length of the laboratory thruster from 8 cm to less than 3 cm is beneficial for bismuth performance. Simulated performance on krypton compared favorably to xenon for the longer 8 cm channel, which compensated for the slightly longer residence time of the lighter propellant. Considering even lighter propellants, such as molecular nitrogen, the otherwise relatively poor performance, due largely to the lower ionization cross section, higher ionization cost, and dramatically lower neutral residence time, can be partly mitigated by a considerable widening of the magnetized region of the plasma, thereby expanding the zone of ionization. Simulated operation on molecular nitrogen clearly indicated a favoring of operation at higher mass flow rates which increases the channel number densities. The results suggest that a further gain might be obtained with nitrogen operation by greatly reducing the channel area.

Acknowledgments

This research was supported in part by the Air Force Office of Scientific Research, with Dr. Mitat Birkan as program manager. Funding for E. Cha was provided by the Samsung Scholarship foundation. Support for M. Scharfe was provided by the National Science Foundation and the Stanford Graduate Fellowship. Support for D. Scharfe was provided by the SGF, NDSEG, and NSF program.

References

[1]Koppel, C. R., and Estublier, D., "The SMART-1 Hall Effect Thruster Around the Moon: In Flight Experience," *29th IEPC,* IEPC-2005-119, Nov. 2005.

[2]Kiechhafer, A., and King, L., B., "Energetics of Propellant Options for High-Power Hall Thrusters," *Proceedings of the Space Nuclear Conference*, 2005.

[3]Scharfe, D. B., "Alternative Hall Thruster Propellants Krypton and Bismuth: Simulated Performance and Characterization," Ph.D. Dissertation, Mechanical Engineering Dept., Stanford University, CA, 2009.

[4]Scharfe, M. K., Thomas, C. A., Scharfe, D. B., Gascon, N, Cappelli, M. A., and Fernandez, E., "Shear-Based Model for Electron Transport in 2D Hybrid Hall Thruster Simulations," *43rd AIAA/ASME/SAE/ASEE Joint Propulsion Conference & Exhibit,* AIAA 2007-5208, Jul. 2007.

[5]Hargus, W. A., Jr., "Investigation of the Plasma Acceleration Mechanism within a Coaxial Hall Thruster," Ph.D. Dissertation, Mechanical Engineering Dept., Stanford University, CA, 2001.

[6]Meezan, N. B., "Electron Transport in a Coaxial Hall Discharge," Ph.D. Dissertation, Mechanical Engineering Dept., Stanford University, CA, 2002.

[7]Fernandez, E., Cappelli, M. A., and Mahesh, K., "2D Simulations of Hall Thrusters," *CTR Annular Research Briefs,* 1998, pp.81, 90.

[8]Fife, J. M., "Hybrid-PIC Modeling and Electrostatic Probe Survey of Hall Thrusters," Ph.D. Dissertation, Dept. of Aeronautics and Astronautics, Massachusetts Institute of Technology, Cambridge, MA, 1998.

[9]Scharfe, M. K., Gascon, N, Cappelli, M. A., and Fernandez, E., "Effect of Charge Exchange on 2D Hall Thruster Simulation," *29th IEPC,* IEPC-2005-057, Nov. 2005.

[10]Thomas, C. A., "Anomalous Electron Transport Barrier in the Hall-Effect Thruster," Ph.D. Dissertation, Mechanical Engineering Dept., Stanford University, CA, 2006.

[11]Bohm, D., Burhop, E., and Massey, H., *The Characteristics of Electrical Discharges in Magnetic Fields*, McGraw Hill, New York, NY, 1949, p.13.

[12]Smith, A. W., and Cappelli, M. A., "Single Particle Simulations of Electron Transport in the Near-Field of Hall Thrusters," *31st IEPC,* IEPC-2009-136, Sept. 2009.

[13]Freund, R. S., Wetzel, R. C., Shul, R. J., and Hayes, T. R., "Cross Section Measurements for Electron-Impact Ionization of Atoms," *Physical Review A*, Vol. 41(7), 3575-3595, Apr. 1990.

[14]Rapp, D., and Englander-Golden, P., "Total Cross Sections for Ionization and Attachment in Gases by Electron Impact. I. Positive Ionization," *The Journal of Chemical Physics*, Vol. 43(5), 1464-1479, Sep. 1965.

[15]Kim, Y.-K., and Rudd, M. E.,"Binary-Encounter-Dipole Model for Electron-Impact Ionization," *Physical Review A*, Vol. 50, 1994.

[16]Hwang, W., Kim, Y.-K., and Rudd, M. E., "New Model for Electron-Impact Ionization Cross Sections of Molecules," *The Journal of Chemical Physics*, Vol. 104(8), pp. 2956, Feb. 1996.

[17]Dugan, J. V. and Sovie, R., J., "Volume Ion Production Costs in Tenuous Plasmas: A General Atom Theory and Detailed Results for Helium, Argon and Cesium," NASA TN D-4150, 1967.

[18]Machereet, S., O., Shneider, M., N., and Murray, R. C., "Ionization in Strong Electric Fields and Dynamics of Nanosecond-Pulsed Plasmas," *Physics of Plasmas*, Vol. 13, 023502, 2006.

[19]Brown S. C., "Chapter 6. Ionization," *Introduction to Electrical Discharges in Gases*, John Wiley & Sons, Inc., pp. 94, 110.

[20]Hagelaar, G. J. M., and Pitchford, L. C., "Solving the Boltzmann Equation to Obtain Electron Transport Coefficients and Rate Coefficients for Fluid Models," *Plasma Sources Science and Technology,* Vol. 14, (2005) 722-733, Oct. 2005.
[21]Meeker, D., http://www.femm.info